



Deposited via The University of Sheffield.

White Rose Research Online URL for this paper:

<https://eprints.whiterose.ac.uk/id/eprint/164399/>

Version: Accepted Version

Article:

Huang, H., Mosalam, K.M. and Chang, W.-S. (2020) Adaptive tuned mass damper with shape memory alloy for seismic application. *Engineering Structures*, 223. 111171. ISSN: 0141-0296

<https://doi.org/10.1016/j.engstruct.2020.111171>

Article available under the terms of the CC-BY-NC-ND licence
(<https://creativecommons.org/licenses/by-nc-nd/4.0/>).

Reuse

This article is distributed under the terms of the Creative Commons Attribution-NonCommercial-NoDerivs (CC BY-NC-ND) licence. This licence only allows you to download this work and share it with others as long as you credit the authors, but you can't change the article in any way or use it commercially. More information and the full terms of the licence here: <https://creativecommons.org/licenses/>

Takedown

If you consider content in White Rose Research Online to be in breach of UK law, please notify us by emailing eprints@whiterose.ac.uk including the URL of the record and the reason for the withdrawal request.

Adaptive tuned mass damper with shape memory alloy for seismic application

Haoyu Huang^a, Khalid M. Mosalam^b, Wen-Shao Chang^{c,*}

^a Beijing Key Lab of Earthquake Engineering and Structural Retrofit, the Key Laboratory of Urban Security and Disaster Engineering of Ministry of Education, Beijing University of Technology, Beijing 100124, China

^b Department of Civil and Environmental Engineering, University of California, Berkeley, CA 94720-1710, USA

^c School of Architecture, University of Sheffield, Sheffield S102TN, UK

* Corresponding author, w.chang@sheffield.ac.uk

Abstract

When the characteristics of the main structure are changed, tuned mass damper (TMD) is easy to meet off-tuning problem. The object of this study is to develop a TMD with shape memory alloy (SMA) to reduce the vibration caused by off-tuning under seismic excitations. By materials characterisation of SMA, when the working temperature rises from -40°C to 65°C , the stiffness increases and the equivalent damping ratio drops. The SMA-based TMD was installed on a steel frame and tested under earthquake loading. The results show the SMA-based TMD is able to reduce the seismic response in the range of 34.09% to 47.77% at the tuned condition. However, by changing the main structural mass, the TMD was easy to be off-tuned. To retune the TMD, the SMA was heated and cooled for the TMD to resonate with the natural frequency of the main structure. When the SMA is cooled, the peak and RMS accelerations can be effectively reduced by up to 23.98% and 35.51%, respectively. It was found that the SMA-based TMD performs well if the frequency change of the main structure is in the same order. But when the temperature of SMA is increased higher than 19°C , the damping ratio of SMA decreases, which causes a less effectiveness in reducing the vibration. In the future, the combinations of multiple SMA bars in TMD should be studied, and the applications of SMAs with higher phase transformation temperature can be investigated to improve the sensitivity while heating.

Keywords

Shape memory alloy; adaptive tuned mass damper; temperature control; off-tune; retune

1. Introduction

To mitigate the structural vibration from dynamic excitations such as wind storms and earthquakes in civil structures, tuned mass damper (TMD) is frequently used in a passive vibration control system. TMD was first proposed in 1909 by Frahm [1] and subsequently developed by Ormondroyd and Den Hartog [2, 3]. TMD has been effectively employed in buildings and bridges in recent years, and examples include Taipei 101 in Taipei, Trump World Tower in New York and Millennium Bridge in London. As shown in Figure 1, a TMD with a mass (m_2), a spring (k_2) and a damper (c_2) can be simulated, being added to an existing structure which has m_1 , k_1 and c_1 as the mass, stiffness and damping of the main structural system. The natural frequency of the TMD should be designed and tuned to a particular range to let the TMD resonate out-of-phase with the main structure [4]. Through this way, the energy can be dissipated effectively by the damping of the TMD and thus the vibration of the main structure is attenuated. The performance and optimal design of the TMD have been studied by previous researchers [5, 6].

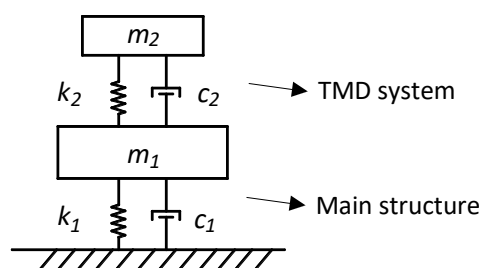


Figure 1 Idealisation of the application of TMD system to a structure

One of the disadvantages of TMD is that it is easy to be off-tuned when the natural frequency of the main structure changes [7]. Instances include increasing/decreasing of the mass on the structure, e.g. due to changes of a building occupancy or a bridge traffic, and stiffness decaying of the structure, e.g. due to inelastic or damaged response [8, 9]. The off-tuned phenomenon could degrade the behaviours of TMD and increase the structural response [10]. In terms of this source of uncertainty, developing a tuneable mass damper with adaptive dynamic characteristics is important. Previous studies have shown that the spring stiffness k_2 and damping coefficient c_2 are able to be adjusted in the TMD so as to bring it back to the tuned condition [7, 11]. Shape memory alloy (SMA) can provide adjustable dynamic characteristics due to its particular thermomechanical properties, and the applications of SMA to TMD have been studied [10]. The previous work has assessed the feasibility of changing the temperature of SMA components in a TMD system to develop a tuneable system [10].

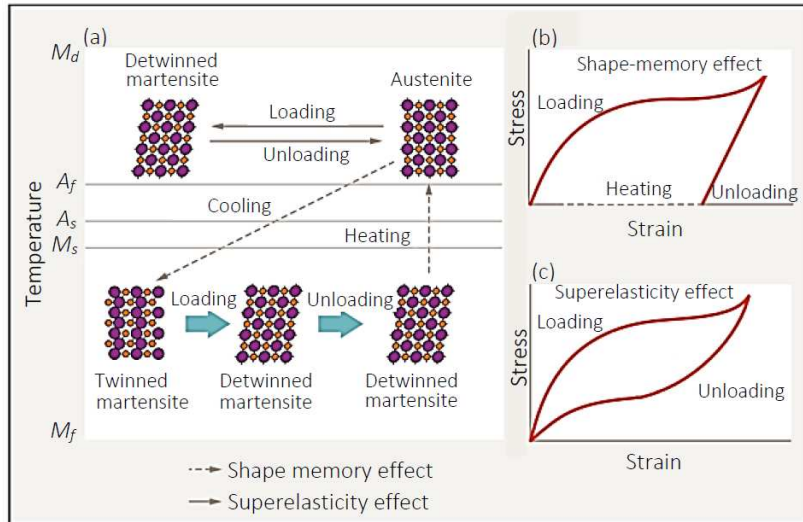


Figure 2 (a) Different phases of SMA at different temperatures and stress-strain curve demonstrating the (b) shape memory effect; (c) superelasticity [12]

SMA is a smart material known as having two unique properties: shape memory effect (SME) and superelasticity, and two phases: martensite and austenite as seen in Figure 2(a) [12]. There are four phase transformation temperatures M_s , M_f , A_s and A_f which indicate the start and finish temperatures of the martensitic and austenitic transformations, respectively, and the mechanical characteristics of the SMA are dependent on them. When the SMA works below its lowest phase transformation temperature (M_f), SMA is in martensitic phase and provides the shape memory effect where its mechanical response undergoes the loading curve in Figure 2(b). In shape memory effect, the SMA recovers to its original shape by external heating; in the view of material science, it transforms from martensite to austenite. Shape memory effect has been studied for repairing and strengthening civil structures [13-15]. When the in-service temperature is higher than the phase transformation temperature, the SMA is in the austenitic phase and superelastic with its hysteresis being self-centering without any external heating, Figure 2(c). The self-centering property of SMA is of significance in the applications to civil structures exposed to extreme winds and earthquakes since it can reduce the damage and residual deformations of structural components and systems [16-18] providing more resilient structural systems. For instance, the superelastic SMA was innovatively studied as bracings for seismic applications [19, 20]. Because of the influence of phase transformation, the mechanical properties of the superelastic SMA can be changed by its working temperature. For example, the transformation stress of SMA increases when temperature goes up [21-23]. Thus, the superelastic SMA can be potentially employed in a TMD to provide adjustable stiffness and damping through controlling temperature.

By controlling the in-service temperature, SMA-based TMDs have been developed in mechanical engineering domain. To increase the adaptability, Williams et al. [24], Aguiar et al. [25] and Rustighi et al. [26] changed the stiffness of the SMA by Joule heating, so as to control the natural frequency of the SMA-based TMD. The results show that the natural frequency of the SMA-based TMD can be adjusted and the effectiveness is enhanced. To avoid the off-tuned situation caused by variable excitation frequencies, Mani and Senthilkumar [27] used multiple SMA springs, and applied both Joule heating and free convection cooling in order to change the natural frequency of SMA-based TMD and the results show that the vibration can be controlled effectively. Elahinia et al. [28] focused on the issue that the change of the primary structural mass can degrade the behaviour of the TMD. For correcting this concern, they adjusted the SMA stiffness by temperature control and the simulation results show that the vibration can be reduced after control. More numerical investigations on tuneable vibration absorber were performed and can be found in [29, 30]. Williams et al. [30] investigated the feasibility of continuously tuned SMA damper. Li et al. [31] developed the SMA-based TMD for tower-line system in order to reduce the seismic vibration. Most previous studies on SMA-based TMD have focused on mechanical engineering applications, and the excitation considered was harmonic vibration or free vibration. Moreover, they examined the effectiveness of SMA-based TMD under single frequency vibration. With respect to civil engineering, the deficiency of previous SMA-based TMD studies is that vibration reduction under earthquakes was not considered in the previous study.

TMD has been extensively studied under the effect of earthquake inputs [32, 33]. SMA-based TMD has the advantages to be applied to earthquake engineering. Under earthquake loading, the material applied to TMD should have stable characteristics and sufficient low-cycle fatigue life. As shown in our material study on SMAs [34], its superelasticity meant that the stress-strain relationship of Cu-Al-Mn SMA was constant during dynamic loading [34]. By contrast, under such a large deformation it is easy for traditional construction material such as steel to have a residual deformation. This could have a substantial effect on its stress-strain relationship and reduce its fatigue life [35]. Another advantage of SMA-based TMD is that it is mechanically simple. The control is based purely on the material phase transformation rather than mechanical operations such as those in SAVIS-TMD [36]. Given the advantages of a SMA, it is important to test the performance of SMA-based TMD under seismic excitations to verify its effectiveness in earthquake engineering. Moreover, unlike machine-induced vibration in mechanical engineering, earthquake involves wider frequency range. Thus, the effectiveness of the SMA retuning ability should be examined. In this study, the performance of a steel

frame mounted with a SMA-based TMD on a shaking table is examined experimentally. The novelty of this paper is that the SMA-based TMD is temperature-controlled in a frequency band, its parameters can be adapted for seismic design, and the aim of the SMA-based TMD is to reduce the earthquake-induced vibration.

2. Free vibration of a SMA bar under different temperatures

In order to develop a tuneable SMA-based TMD used in a structure, essential information, such as stiffness and damping of the SMA in effect of temperatures should be obtained. In the previous work [10], a cantilever beam aligned horizontally with a mass placed at the free end of the beam was used to produce pre-stress effect for free vibration tests in different temperatures. From this previous study, the relationship is established between these properties of the SMA with different pre-stress levels in various working temperatures.

In this study, Cu-Al-Mn SMA (Cu = 81.9%, Al = 7.4% and Mn = 10.7% by weight) provided by Shinko Metal Product Co., LTD, Japan was used. The transformation temperatures of this material were determined by DSC (Differential Scanning Calorimetry) with the result shown in Figure 3. The phase transformation temperatures are determined to be $M_s = -9^\circ\text{C}$, $M_f = -25^\circ\text{C}$, $A_s = -8^\circ\text{C}$ and $A_f = 5^\circ\text{C}$.

The free vibration tests are same with our previous study investigating the effectiveness of SMA-based TMD exposed to wind excitations [37]. The methods and a part of the results illustrated in this section are based on our previous paper [37]. The dynamic characteristics of the SMA-based TMD were obtained by free vibration tests under different temperatures. The analytical model of the SMA-based TMD can be illustrated in Figure 4(a), which is a mass of 6.4 kg hanged through a SMA rectangular bar. The boundary condition is that the top of the SMA bar is fixed on the top floor and the bottom is free and clamped by the mass. It is seen in Figure 4(b) that the middle of the SMA bar is machined to a thin-sheet shape with the cross section of 3×12 mm in order to facilitate the vibration unidirectionally. To prevent the clamping end failure of SMA, the two ends are designed to be thicker. The effective length of the SMA bar is 280 mm as shown in Figure 4. The free vibration tests were initiated by applying a 10 mm horizontal displacement at the free end causing the SMA bar to bend. The free vibration tests were carried out at different temperatures: -40 , -20 , 0 , 19 , 45 , and 65°C of which 19°C represents room temperature. The Tetrafluoroethane sprayings were used on the surface of the SMA bar to cool the specimen to -40 , -20 and 0°C whilst heating was implemented

by wrapping energised carbon fibre, and the heating level was controlled by adjusting the voltage and current of the DC power supply. As conducted in our experimental tests, for SMAs with good thermal conductivity such as copper-based SMA, Tetrafluoroethane sprays can cool the SMA to -40 and -20°C in approximately 1-2 seconds, while heating can be achieved by wrapping the SMA with energised carbon fibre for no more than 5 seconds.

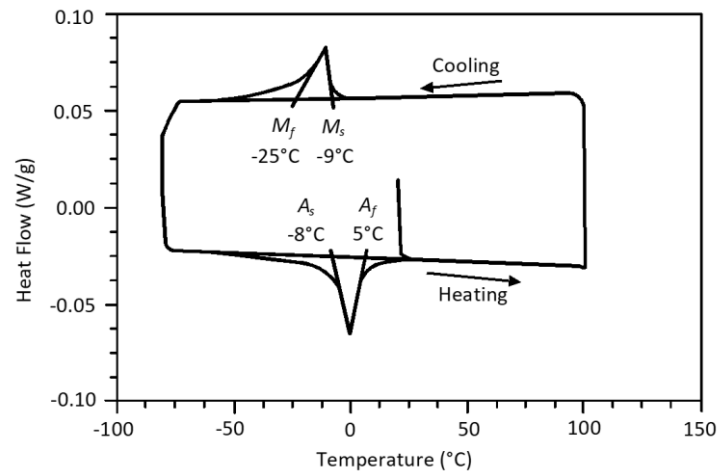


Figure 3 DSC analysis of the SMA sample

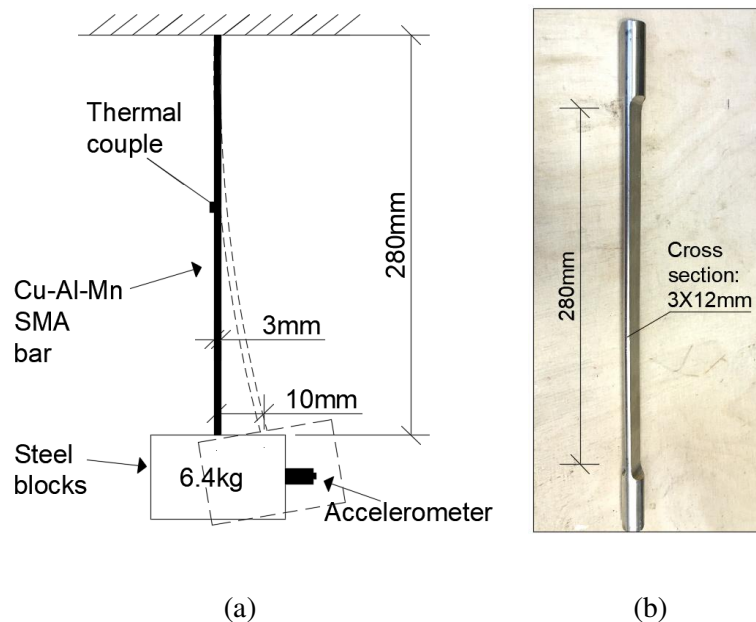
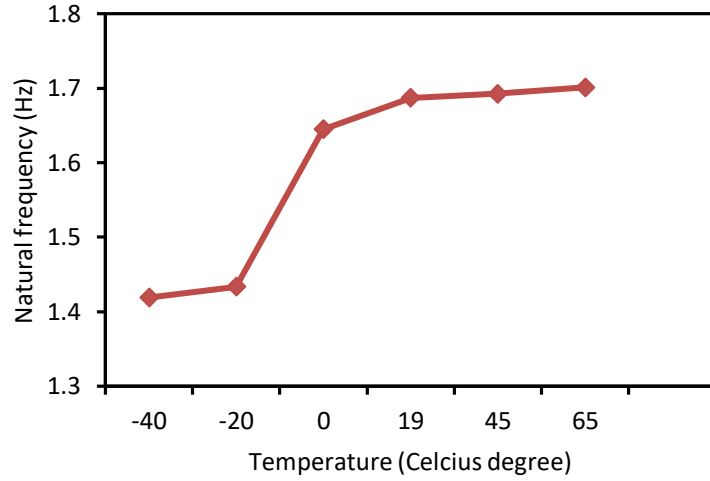
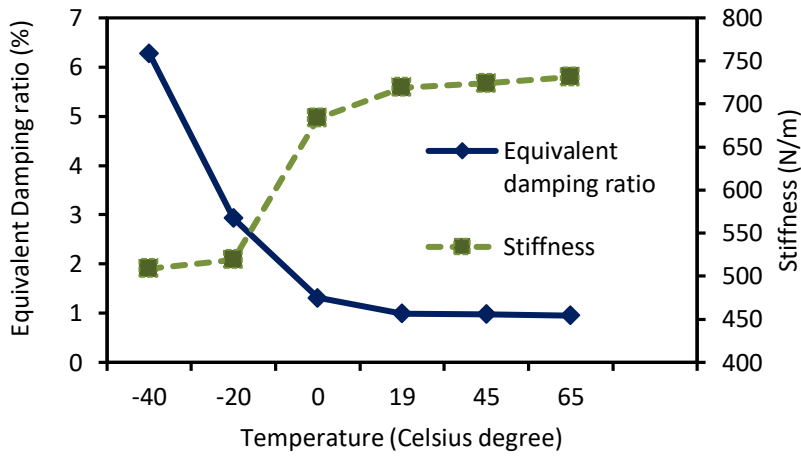


Figure 4 (a) Set-up of single SMA-based TMD free vibration tests (drawing not to scale); (b) Cu-Al-Mn SMA bar [37]



(a)



(b)

Figure 5 (a) Effect of temperature on natural frequency; (b) Effect of temperature on equivalent viscous damping ratio and stiffness [37]

Figure 5 summarises the results of the material tests. Some of the tests results are referred to our previous study in terms of wind excitations [37]. As these data are important to the design of the TMD in this study, they are further discussed in this section. Figure 5 (a) indicates the relationship between natural frequency and temperature. When the temperature rises, the natural frequency increases. In fact, the change of the natural frequency presents the change of the SMA stiffness, as seen in Figure 5 (b) and also in the following equation (1):

$$f = \frac{1}{2\pi} \sqrt{\frac{k}{m}} \quad (1)$$

where f implies the natural frequency, and k and m denote the stiffness and mass, respectively. In Figure 5(b), it is clearly shown that the stiffness of the material increases significantly with the increase of temperature in the range -20 to 0°C, which is in agreement with the phase transformation temperatures, which are in the range -25 to 5°C (Figure 3). The stiffness of the TMD is amplitude-dependent and changeable with the hysteretic loop of SMA. In this study, the dynamic characteristics such as the stiffness and the damping ratio determined for the SMA-based TMD are averaged values including different amplitudes. Figure 5(b) illustrates that the equivalent viscous damping ratio significantly decreases with increasing temperature where the variation is much larger when exposed to cooling than heating. This can be explained by the larger area of hysteresis when the phase approaches martensite. The energy dissipation in cyclic loading is amplitude-dependent. At a high loading amplitude, the energy dissipation of SME is higher than superelastic SMA. At low loading amplitude, the energy dissipation of SME is similar with superelastic SMA as it is in the linear region. In terms of cyclic loading with variable amplitudes like an earthquake, the energy dissipation of SME should be larger than the superelastic SMA.

The temperature range is considered based on the range of the phase transformation temperatures. As seen in Figure 5, the variation of the stiffness and damping intensively occurs in the range of the phase transformation temperatures. In practice, the operating temperature range should cover the range of the phase transformation temperatures, thus SMA is capable to fully transform between the two phases. In other words, the minimum operating temperature should be smaller than M_f , and the maximum operating temperature should be larger than A_f . To achieve a constant stiffness/damping variation, the differences between the max/min temperature and the corresponding phase transformation end temperature should be larger than 20 °C observed by Figure 5. Due to the experimental condition, the SMA cannot be cooled down further than -40 °C while the heating temperature can be easily reached. In applications of SMA-based TMD, SMAs with higher phase transformation temperatures should be used that the adequate cooling can be achieved. Alternatively, more powerful cooling facilities should be employed.

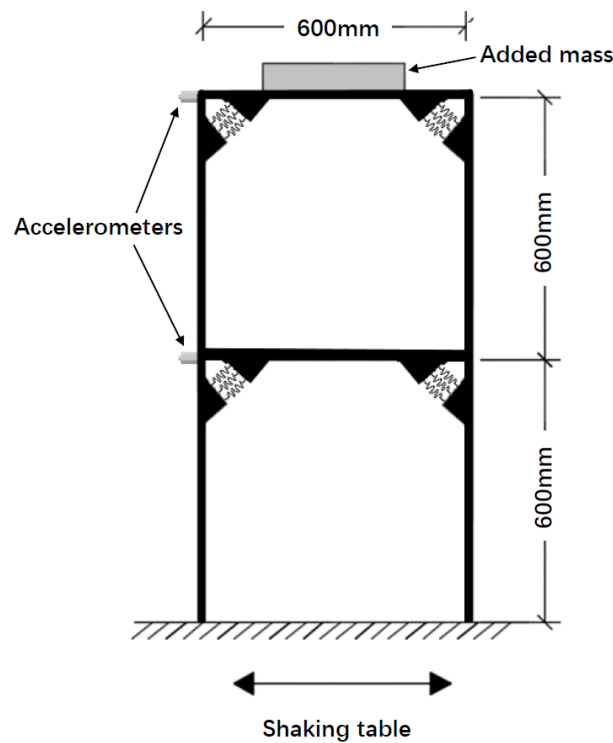
3. Free vibration tests of the main structural system and design of the TMD

To characterise the dynamic properties of the main structure and to assess the feasibility of the TMD design, a reduced-scale steel frame was constructed as the main structure. In this section, the

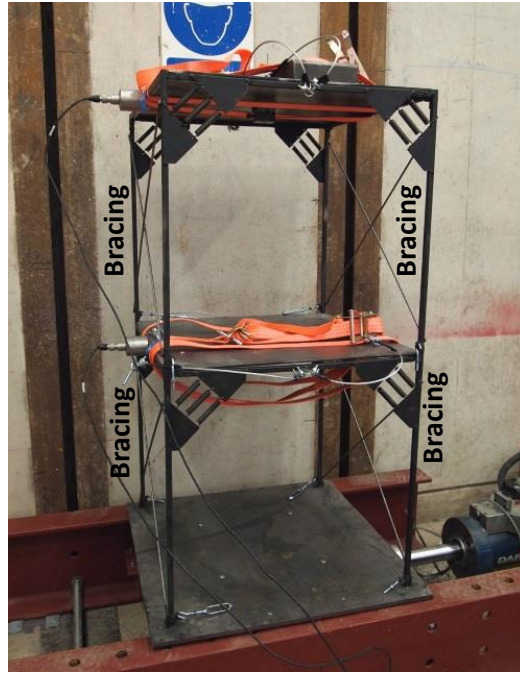
characteristics of the steel frame structure determined from the free vibration tests on a shaking table are discussed. Moreover, the TMD is designed in terms of the characteristics of the main structure.

3.1 Set-up of the main structure: a steel structure system

The main structure used in this study is the same steel framed structure which was used in our previous study investigating the performance subject to wind loadings [37]. The design of the reduced-scale steel framed structure is shown in Figures 6(a) and (b). The steel structure is 1.2 m high and 0.6 m wide, while the dimensions of the slab are 0.6 m \times 0.6 m. The column bases were welded to the shaking table with rigid joints. Figure 6(c) reveals the beam-column connection in detail, where three steel springs are placed in parallel to provide the rotational stiffness. Therefore, the beam-column connections can be modelled as rotational springs. To reduce the vibration in the horizontal direction perpendicular to the seismic excitation, cross bracings were added to each storey, as shown in Figure 6(b). Steel plates were utilised to represent the slabs of the structure which, after examination, were determined to be of sufficient stiffness to model them as rigid diaphragms. A supplementary steel block was added to simulate the mass of the floor, to allow for adjustment of the natural frequency of the structure.



(a)



(b)



(c)

Figure 6 (a) Dimensions of the steel frame [37]; (b) Photograph of the steel frame during testing [37]; (c) Beam-column connection of the steel frame

3.2 Free vibration tests

The natural frequency of the steel frame was characterised by free vibration initiated by a step displacement of 5 mm, provided by the shaking table, as shown in Figure 7(a). Two accelerators were screwed to each floor in order to measure the acceleration with a sampling rate of 100 Hz for a duration of 60 seconds. Figure 7(b) presents the structural response at the top floor with added mass

of 30 kg under free vibration. The natural frequency and damping ratio were calculated from the time domain results using the linear-prediction singular-value decomposition-based matrix pencil (MP) method. For an added mass of 30 kg, the natural frequency of the frame is 1.78 Hz, whilst the semi-active TMD in this study has the natural frequency of 1.68 Hz. For the remainder of the tests, the masses added to the system were 10, 25, 35 and 45 kg, respectively. The natural frequencies of the steel framed structure with different added mass are tabulated in Table 1.

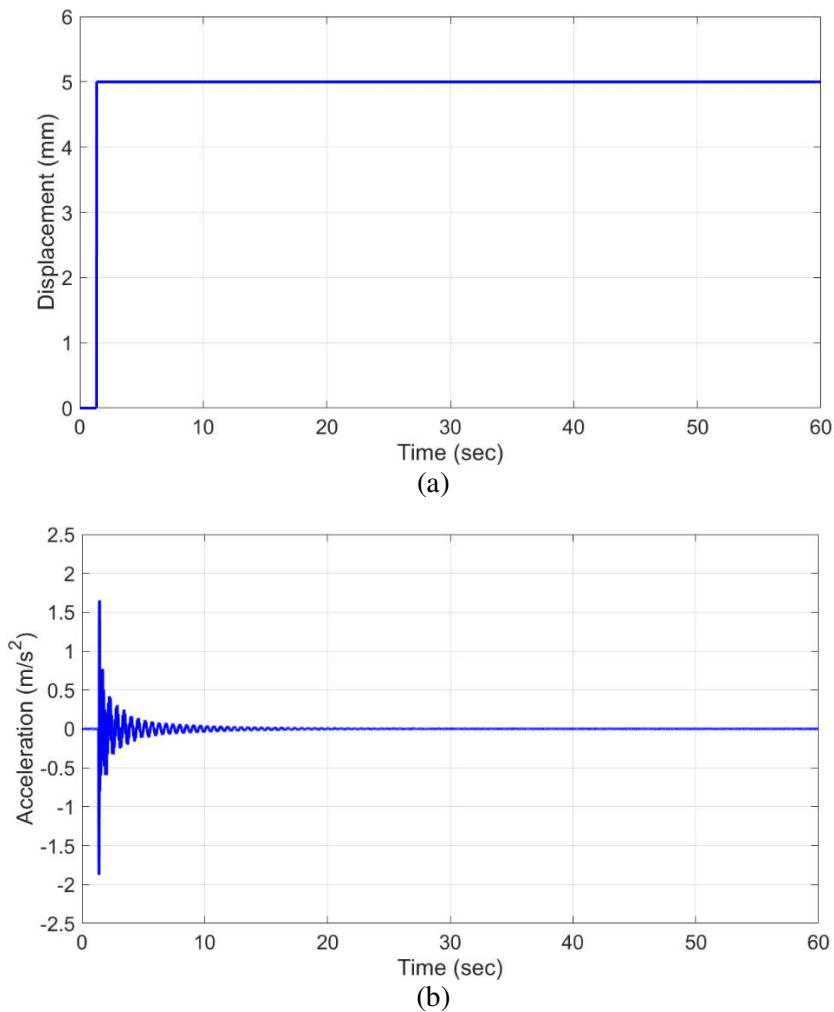


Figure 7 (a) Displacement time history of the shaking table motion; (b) Structural response at the top floor with added mass of 30 kg under free vibration

Table 1 Natural frequencies of the steel frame structure measured by free vibration

Added mass on main structure (kg)	Natural frequency (Hz)
10	2.20
25	1.85
30	1.78
35	1.69
45	1.55

3.3 Design of the TMD

In order for a TMD to be effective, its natural frequency should be approximate to that of the main structure, which enables the TMD to resonate out-of-phase with the main structure. In this regard, several researchers have contributed to the optimisation of TMD design [3, 38-40]. In this study, the design of the TMD is based on the equations proposed by Warburton [38] concerning earthquake excitations, as listed below:

$$f_{opt} = \sqrt{\frac{(1 - \mu/2)}{1 + \mu}} \quad (2)$$

$$\xi_{opt} = \sqrt{\frac{\mu(1 - \mu/4)}{4(1 + \mu)(1 - \mu/2)}} \quad (3)$$

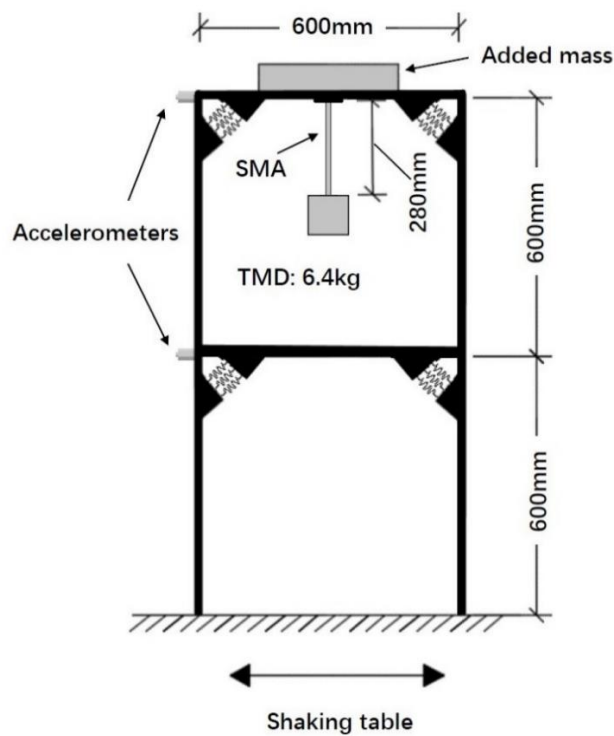
where f_{opt} is the optimal frequency ratio between the natural frequency of the TMD and that of the main structure, ξ_{opt} is the optimal damping ratio of the TMD, and μ is the mass ratio between the mass of the TMD and that of the main structure. Using this analytical model, when the main structure has a natural frequency of 1.78 Hz, the natural frequency of the TMD should be approximately 1.66 Hz, which is close to the measured result of 1.68 Hz, as mentioned above. The dynamic characteristics of the SMA-based TMD including natural frequency, stiffness and damping ratio are presented in Figure 5. By employing Equation (3), the estimated optimal damping ratio ξ_{opt} of the TMD for the structure with added mass of 30 kg is 14.92%, which is larger than 0.99% of the SMA-based TMD. Therefore, the adopted damping ratio of the TMD in this study is not optimally designed. The aim of this study was to reduce the vibration caused by off-tuning. Therefore, the semi-active control was

based on stiffness control and was designed to retune the TMD. Our feasibility study on a cantilever beam [10] showed that off-tuning can drastically increase the vibration amplitude. It is therefore important when controlling the SMA stiffness to bring the TMD into a tuning condition.

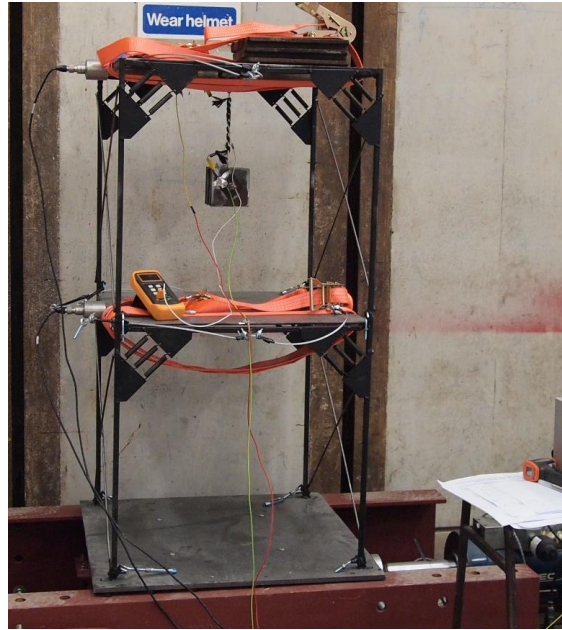
4. Performance of the structure with an off-tuned TMD in shaking table tests

4.1 Methods

The tested Cu-Al-Mn-SMA-based TMD in Section 2 was applied to the steel framed structure, with the installation illustrated in Figure 8. The top of the SMA bar was clamped and fixed to the bottom of the second-storey slab, and the connection was set in a rigid state. Therefore, the stiffness and damping of the TMD contributed to the main structure through the bending of the SMA.



(a)



(b)

Figure 8 Installation of the TMD on the steel frame and shaking table tests set-up: (a) dimensions [37]; (b) photograph taken during the shaking table tests

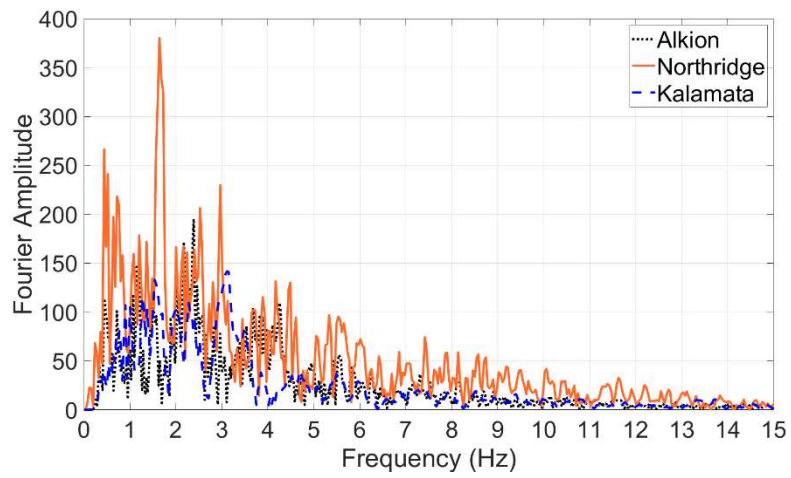


Figure 9 Fourier spectra of the three used earthquake signals

Table 2 Basic information of the three used earthquake signals

Earthquake	The component of the record	Magnitude	Focal depth [km]	Epicentral distance [km]	Peak ground acceleration [m/s ²]	Predominant frequency (Hz)	Date	Location
Alkion	KORINTHOS- OTE BUILDING/E-W	6.8	10	17	3.038	2.38	24 Feb, 1981	Greece
Northridge	Canoga Park- Topanga Can/196 DEG	6.9	19	16	4.042	1.64	17 Jan, 1994	USA
Kalamata	KALAMATA- OTE BUILDING/N10W	5.9	22	73	2.671	3.11	13 Sep, 1986	Greece

In this section, the performance of the steel frame with and without the TMD excited by seismic waves was studied, and the off-tuned performance caused by varying the added mass was investigated. Three earthquake signals were used for input, namely Alkion, Northridge and Kalamata. **The Fourier spectra of these earthquake signals is plotted in Figure 9 by conducting FFT.** The basic information of these records is presented in Table 2. Because of the limitation of the shaking table employed in this study, the input base motion cannot exceed 30 seconds. The three earthquake signals used in this study are selected because they have a shorter duration less than 30 seconds. As a result of the amplitude limits of the shaking table, it was necessary to scale the earthquake waves to 0.125g. The steel framed structure was tested in the conditions with and without the TMD with the added masses, and the test numbers are listed in Table 3.

Table 3 Testing programme of the off-tuned TMD for 60 sec. duration using the three earthquake signals

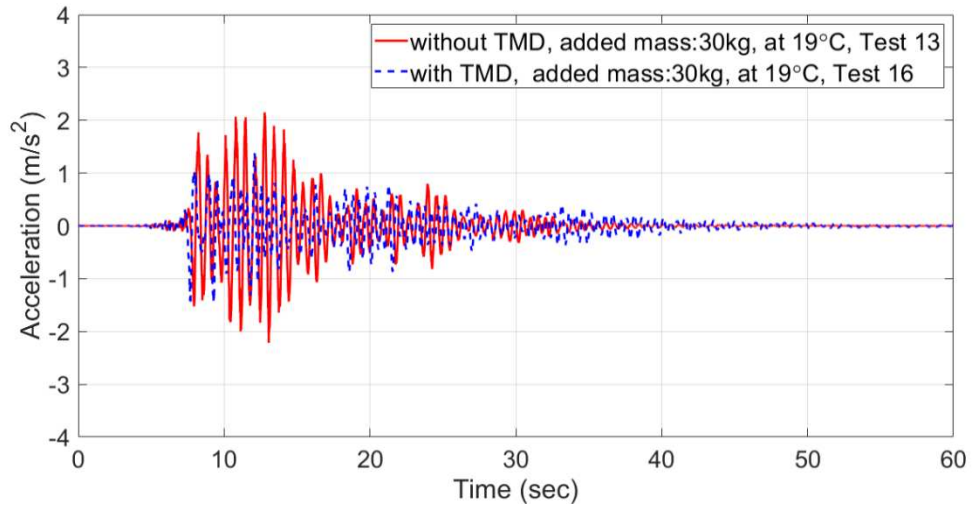
Test number*	Mass added to top floor [kg]	TMD presence
1, 2 and 3	10	Without TMD
4, 5 and 6		With TMD (Frequency ratio**=76.36%, damping ratio=0.99%)
7, 8 and 9	25	Without TMD
10, 11 and 12		With TMD (Frequency ratio=90.81%, damping ratio=0.99%)
13, 14 and 15	30	Without TMD
16, 17 and 18		With TMD (Frequency ratio=94.38%, damping ratio=0.99%)
19, 20 and 21	35	Without TMD
22, 23 and 24		With TMD (Frequency ratio=99.41%, damping ratio=0.99%)
25, 26 and 27	45	Without TMD
28, 29 and 30		With TMD (Frequency ratio=108.38%, damping ratio=0.99%)

*The order of the test numbers corresponds to the application of Alkion, Northridge and Kalamata records.

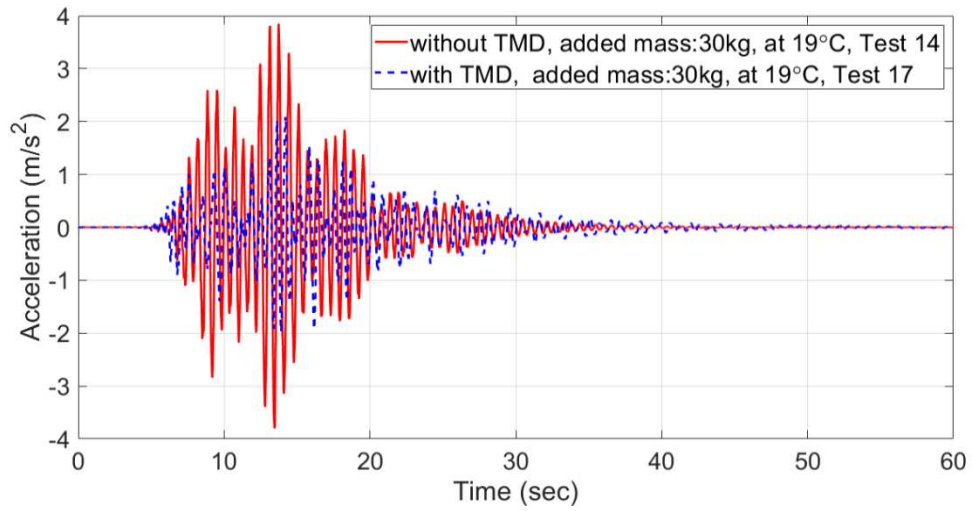
**The frequency ratio means the ratio between the natural frequency of the TMD and the natural frequency of the main structure.

4.2 Discussion

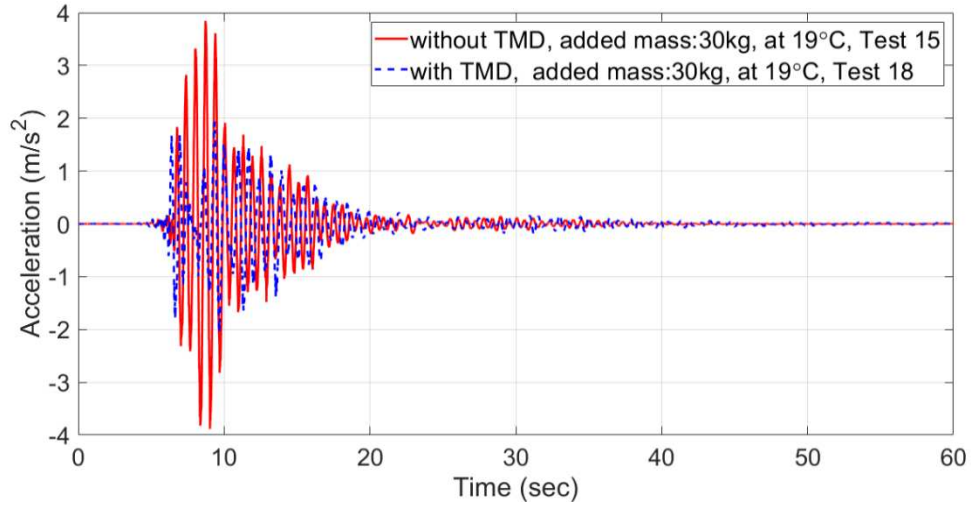
The structural response can be effectively reduced using the TMD with added mass of 30 kg. Figure 10 presents the structural response with the added mass of 30 kg excited by three earthquakes. The structural response under the excitation of Northridge is larger than those under Alkion and Kalamata, because the structural natural frequency (1.78 Hz) is closer to the predominant frequency of Northridge (1.64 Hz). From Figure 10, it can be observed that the structural response with the TMD under earthquake excitation was suppressed to approximately half of that without the TMD. However, after the first 20 sec., the structural response in Test 16 was relatively larger than that in Test 13 at several time instances, as shown in Figure 10(a). This response can be attributed to the damping loss at a smaller amplitude. As the deformation of the SMA is non-linear, the damping ratio of SMA is amplitude-dependent and changeable with the hysteretic loop of SMA. At a lower amplitude, the damping ratio of the SMA is small, thus the energy dissipation capacity is degraded. Therefore, the free vibration of the TMD was not attenuated sufficiently quickly, causing larger vibration to the main structure.



(a)



(b)



(c)

Figure 10 Comparison of the structural response at the top floor with and without TMD excited by (a) Alkion, (b) Northridge and (c) Kalamata

To assess the structural response, the peak acceleration and root mean square (RMS) acceleration at the top floor of each test were tested and the results are presented in Table 4. From Table 4, it is observed that, when the TMD is applied, the smallest peak acceleration was obtained for the condition with an added mass of 30 kg under Alkion and Northridge excitations (Tests 16 and 17). Under the Kalamata excitation, the smallest peak acceleration was obtained in the scenario when a mass of 45 kg was added to the frame (Test 30), rather than the optimum design case for the TMD (Test 18). This is because the natural frequency of the structure with added mass of 45 kg (1.55 Hz) differed more from the predominant frequency of the earthquake (3.11 Hz), as also presented in Test 27, where the peak acceleration was much smaller than that from the remainder of the tests. It is notable, except for Test 30, that the peak acceleration of Test 18 was smaller than that in Tests 12 and 24. From Table 4, it can be observed that the condition where the TMD is applied can effectively reduce the peak structural response under earthquake conditions. In other words, once the main structural mass was changed to an off-tuned state, the peak acceleration increased.

The reduction percentages listed in Table 4 are calculated as follows:

$$Reduction = \frac{(Structural\ response\ without\ damper - Structural\ response\ with\ damper)}{Structural\ response\ without\ damper} \quad (4)$$

Table 4 Peak accelerations (m/s^2) and RMS accelerations (gal)

Earthquake	TMD presence	Mass added to top floor [kg]									
		10		25		30		35		45	
		Peak accelerations (Test #)	RMS accelerations (Test #)	Peak accelerations (Test #)	RMS accelerations (Test #)	Peak accelerations (Test #)	RMS accelerations (Test #)	Peak accelerations (Test #)	RMS accelerations (Test #)	Peak accelerations (Test #)	RMS accelerations (Test #)
Alkion	With TMD	3.196 (4)	58.8 (4)	1.645 (10)	34.4 (10)	1.461 (16)	27.7 (16)	1.527 (22)	24.2 (22)	1.991 (28)	38.3 (28)
	Without TMD	2.934 (1)	55.0 (1)	1.895 (7)	30.2 (7)	2.216 (13)	42.7 (13)	2.047 (19)	41.2 (19)	1.696 (25)	29.1 (25)
	Reduction	-8.95%	-6.91%	13.19%	-13.91%	34.09%	35.13%	25.42%	41.26%	-17.42%	-31.62%
Northridge	With TMD	3.136 (5)	54.9 (5)	2.402 (11)	39.1 (11)	2.084 (17)	38.2 (17)	2.227 (23)	42.0 (23)	2.412 (29)	39.4 (29)
	Without TMD	2.814 (2)	58.9 (2)	5.373 (8)	97.8 (8)	3.851 (14)	72.6 (14)	3.531 (20)	58.1 (20)	3.339 (26)	45.4 (26)
	Reduction	-11.44%	6.79%	55.29%	60.02%	45.88%	47.38%	36.92%	27.71%	27.77%	13.22%
Kalamata	With TMD	3.521 (6)	46.7 (6)	2.068 (12)	33.9 (12)	2.028 (18)	34.4 (18)	2.041 (24)	36.5 (24)	1.786 (30)	29.8 (30)
	Without TMD	4.651 (3)	56.3 (3)	3.806 (9)	64.5 (9)	3.882 (15)	58.5 (15)	3.541 (21)	49.5 (21)	2.505 (27)	49.3 (27)
	Reduction	24.30%	17.05%	45.67%	47.44%	47.77%	41.20%	42.36%	26.26%	28.70%	39.55%

Thus, when the reduction percentage is positive, it implies that the TMD played an effective role and successfully reduced the structural response. The results in Table 4 demonstrate that the TMD can reduce the structural peak acceleration in the range of 34.09% to 47.77% at the tuned condition. With the added masses of 10 kg and 45 kg under Alkion excitation and with the added mass of 10 kg under Northridge excitation, the structural response was increased by up to 17.42% by using the TMD. This observation implies that the TMD is off-tuned, which instigates an increased structural response and presents significant risks to the structure when subjected to earthquake conditions.

The RMS accelerations were reduced to minimal levels through application of the TMD at a tuned condition (added mass = 30 kg) under all three earthquake excitations according to the data from Tests 16, 17 and 18 in Table 4. When the structure was excited under Northridge earthquake conditions in Test 17, the RMS acceleration was lowest when using the TMD at the tuned condition, illustrating the effectiveness with an overall decrease of the structural response after using the TMD. When the

structure was excited under Alkion and Kalamata earthquake excitations, the RMS accelerations were at their lowest under 35 kg and 45 kg added mass conditions, respectively. This is attributed to the fact that the TMD in this study was not designed to have an optimal damping ratio and its damping ratio was lower than the theoretical design value. The low damping of the TMD could result in larger vibration, which may degrade the effectiveness of the TMD in free vibration. Thus, the low damping of the TMD influenced the RMS results.

5. Retuned TMD by changing the SMA temperature under seismic excitations

Considering the particular thermomechanical properties of SMAs, the natural frequency and damping ratio of a SMA-based TMD can be adjusted by modifying the temperature. In this section, a SMA-based TMD is employed in a steel framed structure in order to reduce the structural seismic response caused by off-tuned conditions.

5.1 Control method

As presented in Figure 11, a semi-active control method is used for the SMA-based TMD, which means that changes in the modal properties of the main structure are first determined, and the TMD parameters are adjusted subsequently to adapt to these new properties. In other words, the tuned condition of a system can be preserved when the mass of the main structure increases owing to a reduction in the stiffness of the TMD. Conversely, as the mass of the main structure decreases, the stiffness of the TMD should increase. The aim of the control method is to adjust the TMD into an optimal condition for seismic vibration reduction after detecting the main structural modal properties. According to Sections 2 and 3, when the added mass is changed to 25 kg and 45 kg, the theoretically estimated natural frequency of the TMD in each case should be 1.713 Hz and 1.464 Hz, respectively. To achieve these estimated natural frequencies of 1.464 Hz and 1.713 Hz, the SMA should be cooled to approximately -25°C and heated to approximately 65°C , as inferred from Figure 5(a). The heating and cooling methods are same with those illustrated in Section 2. The testing programme of the steel frame in this case is documented in Table 5, where the procedures and acceleration measurements of these shaking table tests are similar to those discussed in the previous section. As shown in Table 4, the peak acceleration with added mass of 45 kg in Test 30 was low. Thus, under seismic excitations equivalent to the Kalamata earthquake, the added mass was increased to 35 kg in order to off-tune the TMD, as indicated in Table 5.

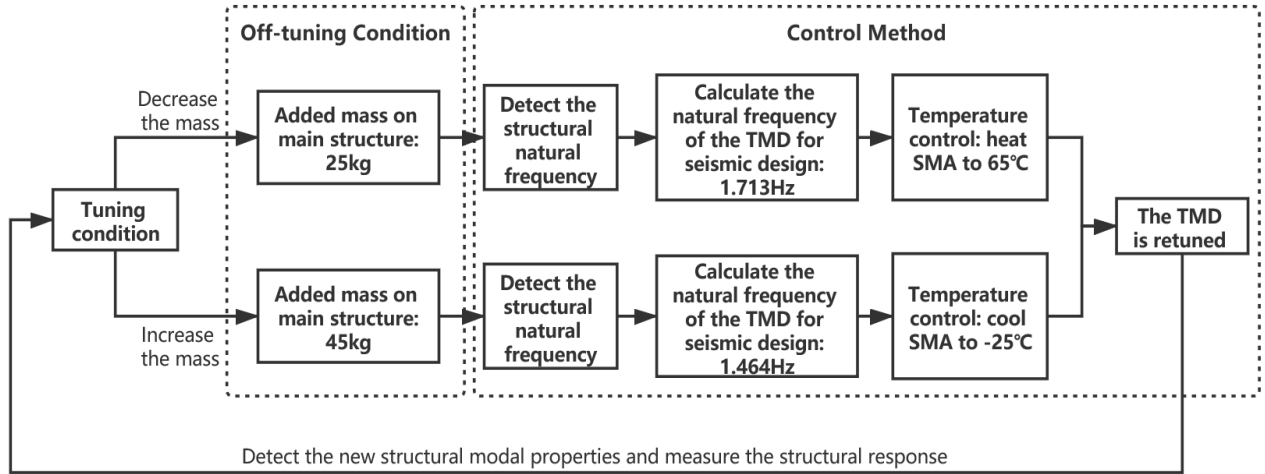


Figure 11 Control method of the SMA-based TMD in this study

Table 5 Testing programme of the retuning runs for 60 sec. duration using the three earthquake signals

Test number*	Mass added to top floor [kg]	TMD conditions
31, 32 and 33	Increase mass to 45 kg (Alkion & Northridge) or 35 kg (Kalamata)	Decrease temperature to -20°C
34, 35 and 36		Decrease temperature to -40°C
37, 38 and 39	Decrease mass to 25 kg	Increase temperature to 45°C
40, 41 and 42		Increase temperature to 65°C

*The order of the test numbers corresponds to the application of Alkion, Northridge and Kalamata records.

Table 6 Changes of the peak and RMS accelerations after increasing the added mass on the main structure

Earthquake	Acceleration	Accelerations for mass added to top floor [kg] (Test #)		Increase
		30 (All)	45 for Alkion & Northridge and 35 for Kalamata	
Alkion	Peak [m/s ²]	1.461 (16)	1.991 (28)	36.32%
	RMS [gal]	27.7 (16)	38.3 (28)	38.27%
Northridge	Peak [m/s ²]	2.084 (17)	2.412 (29)	15.72%
	RMS [gal]	38.2 (17)	39.4 (29)	3.14%
Kalamata	Peak [m/s ²]	2.028 (18)	2.041 (24)	0.66%
	RMS [gal]	34.4 (18)	36.5 (24)	6.10%

5.2 Retuning the TMD when the structural mass increases

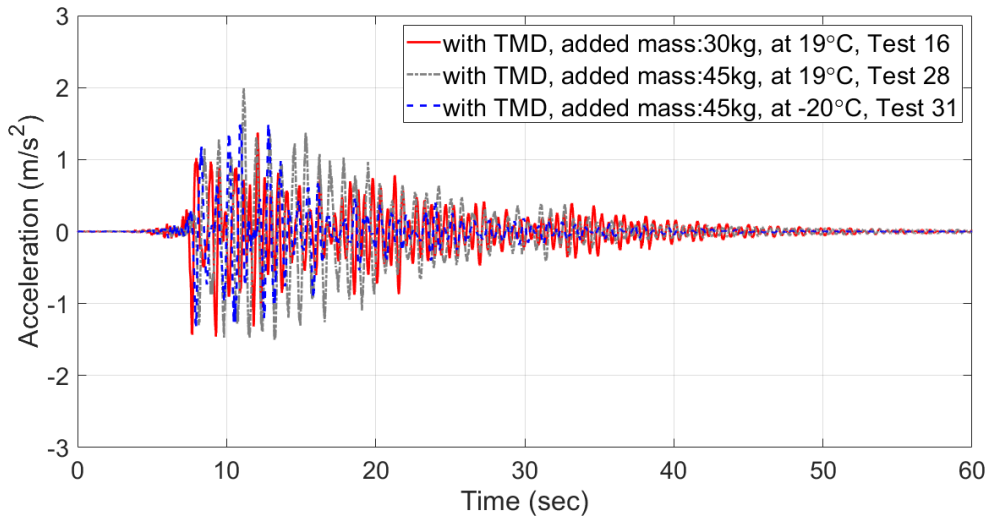
Before analysing the effect of temperature control of the SMA-based TMD, the problems caused by increasing the structural response due to increasing the mass of the main structure should be highlighted. In Table 6, the peak and RMS accelerations at the top floor are presented. The percentage increases of the structural response by increasing the mass are 36.32% in the peak acceleration and 38.27% in the RMS acceleration under the Alkion earthquake excitation.

To reduce the increasing vibration, SMA cooling was conducted in order to retune the TMD. After cooling the SMA to -20°C and -40°C , as shown in Figure 12, the structural response at the top floor was effectively reduced. It can be observed that the response with the retuned TMD (Tests 31 and 32) can be reduced to a comparable level in which the tuned passive TMD was employed (Tests 16 and 17). Moreover, the vibration can be attenuated more efficiently when compared with the system without temperature control. In Table 7, it is demonstrated that the peak and RMS accelerations can be reduced by up to 23.98% and 35.51%, respectively. Under the excitations of the Northridge earthquake, the peak acceleration using the cooling SMA-based TMD can be controlled to 1.885m/s^2 , which is lower than the result of 2.084 m/s^2 for the tuned condition. The RMS acceleration was also reduced to a lower level by cooling the TMD than the tuned condition. This can be explained by the fact that cooling the SMA results in increased damping, which reduces the free vibration of the TMD caused by off-tuning. When the SMA is cooled down, the structural natural frequency decreases and differs from the predominant frequency of the Kalamata earthquake (3.11 Hz), which leads to a smaller structural response reduction (Tests 33 and 36). In summary, the results show that retuning the TMD by cooling the SMA can effectively attenuate the increased vibration resulting from the off-tuned scenarios. It was also found that the SMA-based TMD performs well if the frequency change of the main structure is in the same order.

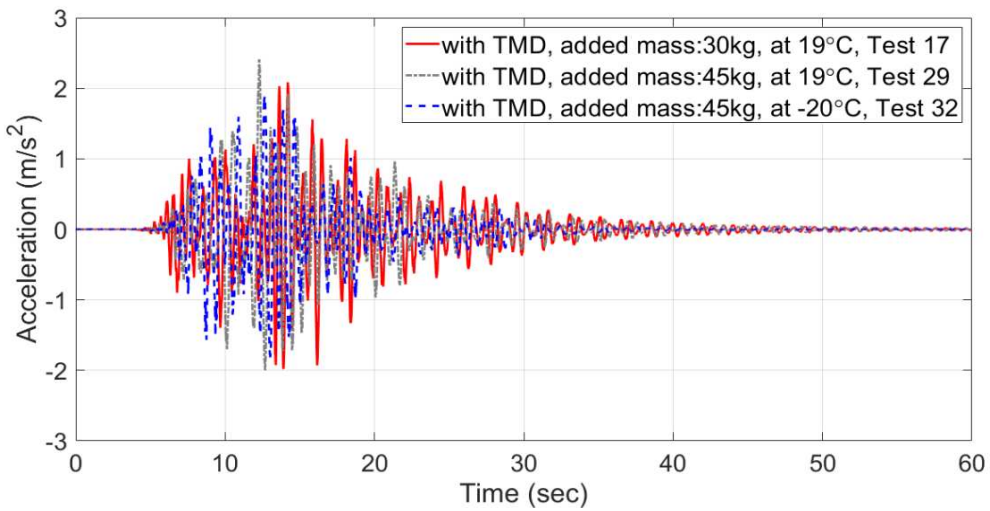
It should be noted that the SMA deforms in martensite when the temperature is -20°C . However, the residual strain caused by the martensite can be reduced to a neglect level after the action, which are attributed to two reasons. Firstly, the SMA-based TMD was vertically placed, and the hanged mass forced the SMA bar to possess a straight form due to the gravity. Secondly, when the temperature increased to the ambient temperature, the deformation was self-centred as presented in the Figure 2 (b).

Table 7 The structural response with added mass of 45 kg (Alkion and Northridge) and 35 kg (Kalamata) after re-tuning the TMD by cooling the SMA

Earthquake	TMD Temperature [°C]	Test #	Acceleration	Reduction
			Peak [m/s ²]	
Alkion	-40	34	1.524	23.45%
	-20	31	1.514	23.98%
	19	28	1.991	Reference
			RMS [gal]	
	-40	34	24.7	35.51%
	-20	31	25.0	34.73%
	19	28	38.3	Reference
			Peak [m/s ²]	
Northridge	-40	35	1.975	18.11%
	-20	32	1.885	21.85%
	19	29	2.412	Reference
			RMS [gal]	
	-40	35	35.6	9.64%
	-20	32	35.2	10.66%
	19	29	39.4	Reference
			Peak [m/s ²]	
Kalamata	-40	36	2.038	0.14%
	-20	33	2.067	-1.29%
	19	24	2.041	Reference
			RMS [gal]	
	-40	36	34.3	6.03%
	-20	33	34.6	5.20%
	19	24	36.5	Reference



(a)



(b)

Figure 12 Comparison of the structural response at the top floor with TMD between 19°C & -20°C with added mass of 45 kg and 30 kg and excited by (a) Alkion and (b) Northridge

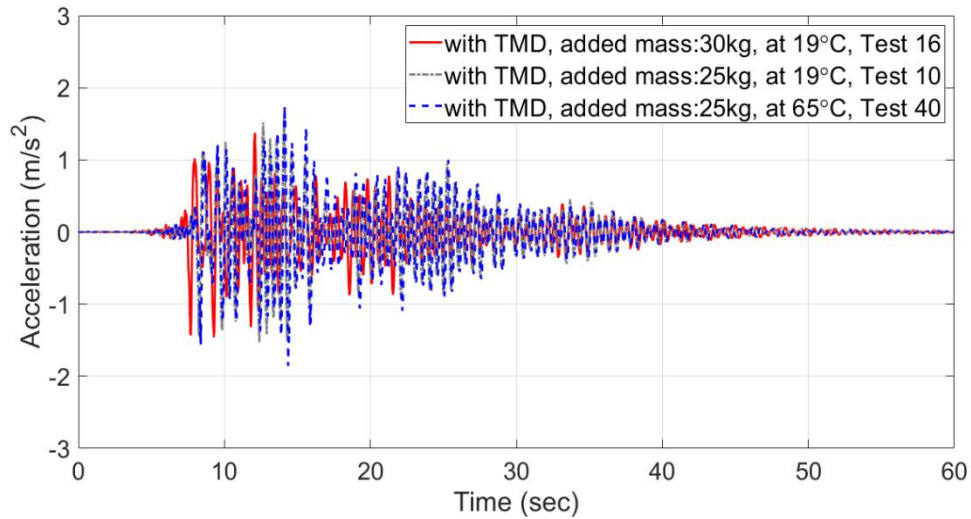
5.3 Retuning the TMD when the structural mass decreases

When the main structural mass decreases, the TMD becomes off-tuned and the structural response tends to be larger. As seen in Table 8, the peak and RMS accelerations measured from the top floor indicate that the peak acceleration increases by 12.60% and its RMS acceleration increases by 24.19%.

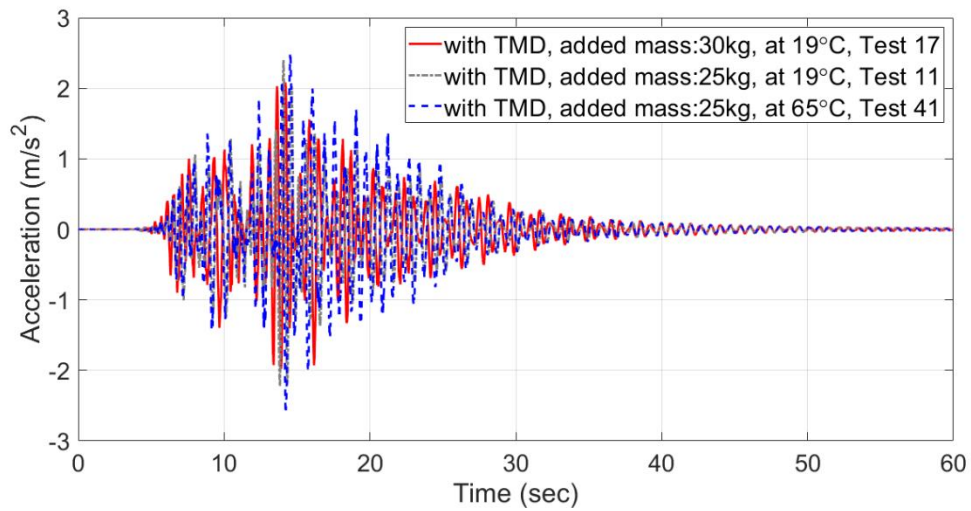
Table 8 Changes in the peak and RMS accelerations after decreasing the added mass on the main structure

Earthquake	Acceleration	Accelerations for mass added to top floor [kg] (Test #)		Increase
		30	25	
Alkion	Peak [m/s ²]	1.461 (16)	1.645 (10)	12.60%
	RMS [gal]	27.7 (16)	34.4 (10)	24.19%
Northridge	Peak [m/s ²]	2.084 (17)	2.402 (11)	15.26%
	RMS [gal]	38.2 (17)	39.1 (11)	2.36%
Kalamata	Peak [m/s ²]	2.028 (18)	2.068 (12)	1.98%
	RMS [gal]	34.4 (18)	33.9 (12)	-1.45%

The temperature of the SMA was increased to 45°C and 65°C in order to retune the TMD. Figure 13 describes the main structural response at the top floor. It is observed that the vibration was not reduced and even increased in some instances after heating the SMA to 65°C. As presented in Figure 13, the structural response with retuned TMD was not reduced to the level in which the tuned passive TMD is applied. From the assessment using the peak and RMS accelerations, in most cases, these accelerations increased a little by raising the SMA temperature. Therefore, the effectiveness of retuning by heating the SMA is limited, and there are two principle explanations for this performance. According to Figure 5(b), the equivalent viscous damping ratio of the SMA reduces by increasing the temperature, and this damping loss can increase the free vibration. Furthermore, the variation of the SMA stiffness at a temperature greater than 19°C is low, which provides limited adaptivity for it to be utilised for the purpose of retuning.



(a)



(b)

Figure 13 Comparison of the structural response at the top floor with a TMD between 19°C & 65°C with added mass of 25 kg and 30 kg and excited by (a) Alkion and (b) Northridge

5.4 Discussion and future extensions

The limited efficiency of heating SMA can be attributed to the reduction of damping ratio while heating SMA. Lower damping could cause the vibration response larger, because reduction of the damping leads to a narrow effective frequency bandwidth of TMD. Through the analysis of the results in previous study [10], it can be deduced that increasing the SMA temperature to retune the TMD with the main structure can only be effective at a narrow frequency range. This system could be utilised in

mechanical engineering applications in order to reduce machine-induced vibrations. However, in terms of their applications in earthquake engineering, TMDs are required to be effective in a broad range of frequencies. Optimisation of the SMA-based TMD can be achieved by employing more than one SMA bar, as discussed by Williams, Chiu [24]. According to the theory illustrated by Meirovitch [41], when multiple SMA bars are applied together in parallel, the stiffness and damping can be combined. This configuration allows for heating and cooling of different bars within the system concurrently. Thus, both stiffness and damping can be controlled. In other words, by combining multiple bars when the natural frequency of the TMD is tuned, the damping ratio can be adjusted to a satisfactory level. This control theory will be investigated in further studies. In terms of practicality, heating can reduce the damping ratio of the SMA, as shown in Figure 5 (b). To enhance the damping ratio under heating, the SMA can be installed in a pre-strained form. In our previous studies [35, 42], experiments showed that pre-strained SMAs can significantly increase the damping ratio. This solution ensures the SMA has sufficient damping.

The contribution of this study is that a temperature-controlled SMA-based TMD system is developed for seismic applications, and it has potential to be commercially employed in real engineering projects. The hypothesis of this study is that the off-tuned structure can be retuned by the SMA-based TMD using temperature control. In terms of the results, changing SMA's temperature by cooling can retune the natural frequency of TMD and can also increase the damping capacity, which is effective in the seismic reduction control. To contribute the engineering applications using the results obtained in this study, it is important to investigate how a real structure determines when retuning is required. Under earthquake action, the excitation is random and in a wide frequency bandwidth. The SMA-based TMD has the potential to control the earthquake-induced vibration, because the structural dynamic characteristics can be adapted to avoid the resonance with the predominant frequency of the earthquake. In this study, only two distinct off-tuning conditions are investigated. In the future extensions, a structural control system with sensors can be developed. These sensors could measure the structural response and report to a computer controlling system in cases of frequency shift. Through analysis of the frequency shift, the optimum temperature required is returned to the SMA components from the controlling system, which consequently enables adjustments to the optimal parameters of the TMD through heating and cooling. Thermocouples should be applied on SMAs in order to measure the temperature and provide feedback to the controller for continuous heating or cooling. For seismic applications, the algorithms of the controlling system should be simplified to enable rapid response in cases of high-frequency loadings, all of which requires further investigation.

The faster heating/cooling techniques and SMAs with high thermal conduction should be investigated as well. After the earthquake or a long period of usage, it should be noted that the structure may be degraded and the stiffness may decrease, which causes a lower structural natural frequency. The semi-active control method developed in this study can adaptively tune the structural natural frequency in the specific range. If the structural natural frequency is reduced in a large amount and beyond the tuneable range of the SMA-based TMD, the extra SMA bars can be disassembled under the premise of a sufficient strength so as to achieve the lower natural frequency of the TMD. **During the earthquake, the stiffness of the structure may change and it could influence the effectiveness of the TMD. It is vital to govern this change of the stiffness of the structure due to the manifestation of inelastic behaviour. Tsiavos and Stojadinovic [43] proposed a novel procedure for the seismic assessment of structures, defined as Constant Yield Displacement Evaluation (CYDE). This procedure is based on the preservation of the yield displacement of a structure as the fundamental principle that governs the change of the stiffness of the structure during a variation of its strength. In case of stiffness changing, the retuning of the SMA-based TMD based on the CYDE principle should be investigated numerically and experimentally in the future study.**

To apply this temperature controlled SMA-based semi-active TMD to civil engineering, scaling to actual civil structures must be undertaken as this study was conducted on a laboratory scale. When using large-scale structures, large-size SMA bars should be employed to provide a large force and render this TMD feasible in practice. In line with the development of the material manufacturing process, the abnormal grain growth (AGG) method as a thermomechanical treatment has been implemented to produce Cu-Al-Mn SMA bars whose grain size is larger than the diameter [44]. The 'bamboo-like' grain structure [34] can reduce the constraints of the polycrystalline structure and improve superelasticity. The resulting improvement of SMA fabrication and thermomechanical treatment means that it is now possible to produce large-size SMA bars with a diameter of up to 30 mm. Two Japanese material companies, Furukawa Techno Material Co., Ltd. and Shinko Metal Products Co., Ltd, have strived to improve the manufacturing methods and produce Cu-Al-Mn bars on a large scale. This is because copper is cost-effective and exhibits good cold workability and machinability [44, 45]. Overall, it is now possible for large-size SMA bars to be manufactured for use in construction. These bars can also be installed in parallel which means their stiffness can be combined and increased, making them suitable for real-life civil engineering applications.

One of the first applications of TMD was the 60-story John Hancock building in Boston in 1977, which has two 300-ton TMDs. Taipei 101 employed a TMD with a weight of 660 tons connected by 16 ropes, each 9 mm in diameter. In high-rise buildings, the TMD weight and connecting elements are large in size. To vary the in-service temperature of the SMA in a full-scale TMD system, the temperature control should be as rapid as that in the laboratory tests. The thermal conductivity of copper is 4.4 times that of nickel and 18.2 times that of titanium, therefore a copper-based rather than NiTi SMA is preferred for temperature control on a large scale. Thus, heating by wrapping energised wires and cooling by freezing sprays is more applicable. It is important to note that, as illustrated in Figure 5(b), the sensitivity of the SMA to temperature is significant, especially as it approaches the phase transformation temperature. When these phase transformation temperatures are set close to the working temperature, slight adjustments can drastically vary the stiffness and damping ratio. Such phase transformation temperatures can therefore be selected and applied to the SMA-based TMD system to improve the effectiveness of the temperature control. In cases where an extremely large SMA element is used, this can be replaced by several smaller-sized SMA elements in parallel. The temperature control on the SMA can therefore be eased by reducing the scale.

With regard to the application of SMAs, stabilisation should be considered. The damping ratio and stiffness of the SMA are not stable and are expected to decrease gradually in the early loading cycles [22, 46-51]. This could influence the accuracy of the intended structural control. Pre-training of the SMA should be conducted by static cyclic loading before use, so as to stabilise the obtained dynamic properties.

6. Conclusions

To reduce the vibration caused by off-tuned TMD, SMA was applied to retune the TMD using temperature control. Before the application to structures, a single SMA-based TMD was characterised at different temperatures. The results show that the stiffness increases and the equivalent damping ratio decreases with rising temperature from -40°C to 65°C . Thus, the dynamic characteristics of the TMD are adjustable.

A steel frame structure was designed such that the TMD can tune, and the SMA-based TMD developed in this study was installed. Then, the structure was tested on a shaking table under three earthquake excitations. Based on the results, the following conclusions can be drawn:

- At the tuned condition, the structural response can be effectively reduced with the TMD.
- The peak and RMS accelerations were found to be increased when the tuned condition is broken.
- When the added mass on the main structure increased, the tuneable mass damper was subjected to cooling leading to the decrease of the stiffness and natural frequency. Presented results showed that the peak and RMS accelerations can be effectively reduced up to 23.98% and 35.51%, respectively, under the excitation of earthquakes.
- When the structural mass was decreased, heating SMA was conducted to retune the TMD. However, in most cases, the effectiveness of heating the SMA-based TMD was limited. This is attributed to the fact that the damping reduces while heating and the variations of the dynamic properties are small at higher temperature than 19°C.

To improve the retuning ability of using SMA heating, the combinations of multiple SMA bars can be studied, and SMAs with higher phase transformation temperature can be employed in future studies. The combinations of multiple SMAs and increasing the phase transformation temperatures of SMA can optimise the damping ratio of the SMA-based TMD.

Acknowledgement

The authors would like to thank funding from National Natural Science Foundation of China (51908007), Beijing Municipal Education Commission (KM201910005021), Basic Research Foundation of Beijing University of Technology and International Copper Association (TEK-1079). The authors also thank Shinko Metal Product Co., LTD for their shape memory alloy supply.

Reference

- [1] Frahm H. Device for damping vibrations of bodies. U.S.1909.
- [2] Ormondroyd J, Den Hartog JP. The theory of dynamic vibration absorber. *Journal of Applied Mechanics Trans ASME*. 1928;50:9-22.
- [3] Den Hartog JP. *Mechanical vibrations*. 4th ed. New York ; London: McGraw-Hill; 1956.
- [4] Connor JJ. *Introduction to structural motion control*. Upper Saddle River, N.J.: Prentice Hall Pearson Education, Inc.; 2003.
- [5] Warburton GB. Optimum Absorber Parameters for Various Combinations of Response and Excitation Parameters. *Earthquake Eng Struc*. 1982;10:381-401.
- [6] Sadek F, Mohraz B, Lew HS. Single- and multiple-tuned liquid column dampers for seismic applications. *Earthquake Engineering & Structural Dynamics*. 1998;27:439-63.
- [7] Nagarajaiah S, Sonmez E. Structures with semiactive variable stiffness single/multiple tuned mass dampers. *J Struct Eng-Asce*. 2007;133:67-77.
- [8] Xue S, Tang H, Okada J, Hayashi T, Zong G, Arikawa S. Natural frequency changes for damaged and reinforced real structure in comparison with shake table and simulation. *Materials forum*. 2009;33:344-50.

- [9] Brincker R, Rodrigues J, Andersen P. Scaling the mode shapes of a building model by mass changes. IMAC-22: A Conference on Structural Dynamics. Hyatt Regency Dearborn, Dearborn, Michigan, USA: Society for Experimental Mechanics; 2004. p. 119-26.
- [10] Huang HY, Chang WS, Mosalam KM. Feasibility of shape memory alloy in a tuneable mass damper to reduce excessive in-service vibration. *Struct Control Hlth*. 2017;24:1-14.
- [11] Sun C, Eason RP, Nagarajaiah S, Dick AJ. Hardening Duffing oscillator attenuation using a nonlinear TMD, a semi-active TMD and multiple TMD. *J Sound Vib*. 2013;332:674-86.
- [12] Chang W-S, Araki Y. Use of shape-memory alloys in construction: a critical review. *Proceedings of the Institution of Civil Engineers - Civil Engineering*. 2016;169.
- [13] Li H, Liu ZQ, Ou JP. Behavior of a simple concrete beam driven by shape memory alloy wires. *Smart Mater Struct*. 2006;15:1039-46.
- [14] Choi E, Nam TH, Cho SC, Chung YS, Park T. The behavior of concrete cylinders confined by shape memory alloy wires. *Smart Mater Struct*. 2008;17.
- [15] Choi E, Chung YS, Cho BS, Nam TH. Confining concrete cylinders using shape memory alloy wires. *Eur Phys J-Spec Top*. 2008;158:255-9.
- [16] Choi E, Lee DH, Choei NY. Shape memory alloy bending bars as seismic restrainers for bridges in seismic areas. *Int J Steel Struct*. 2009;9:261-73.
- [17] Alam MS, Nehdi M, Youssef MA. Seismic performance of concrete frame structures reinforced with superelastic shape memory alloys. *Smart Struct Syst*. 2009;5:565-85.
- [18] Chang WS, Murakami S, Komatsu K, Araki Y, Shrestha K, Omori T et al. Technical Note: Potential to Use Shape Memory Alloy in Timber Dowel-Type Connections. *Wood Fiber Sci*. 2013;45:330-4.
- [19] Qiu C-X, Zhu S. Performance-based seismic design of self-centering steel frames with SMA-based braces. *Eng Struct*. 2017;130:67-82.
- [20] Qiu C, Zhu S. Shake table test and numerical study of self-centering steel frame with SMA braces. *Earthquake Engineering & Structural Dynamics*. 2017;46:117-37.
- [21] Araya R, Marivil M, Mir C, Moroni O, Sepulveda A. Temperature and grain size effects on the behavior of CuAlBe SMA wires under cyclic loading. *Materials science and engineering A - structural materials properties microstructure and processing*. 2008;496:209-13.
- [22] Dolce M, Cardone D. Mechanical behaviour of shape memory alloys for seismic applications - 2. Austenite NiTi wires subjected to tension. *Int J Mech Sci*. 2001;43:2657-77.
- [23] Andrawes B, DesRoches R. Effect of ambient temperature on the hinge opening in bridges with shape memory alloy seismic restrainers. *Engineering structures*. 2007;29:2294 - 301.
- [24] Williams K, Chiu G, Bernhard R. Adaptive-passive absorbers using shape-memory alloys. *J Sound Vib*. 2002;249:835-48.
- [25] Aguiar RAA, Savi MA, Pacheco PMCL. Experimental investigation of vibration reduction using shape memory alloys. *J Intel Mat Syst Str*. 2013;24:247-61.
- [26] Rustighi E, Brennan MJ, Mace BR. Real-time control of a shape memory alloy adaptive tuned vibration absorber. *Smart Mater Struct*. 2005;14:1184-95.
- [27] Mani Y, Senthilkumar M. Shape memory alloy-based adaptive-passive dynamic vibration absorber for vibration control in piping applications. *J Vib Control*. 2015;21:1838-47.
- [28] Elahinia MH, Koo JH, Tan H. Improving robustness of tuned vibration absorbers using shape memory alloys. *Shock Vib*. 2005;12:349-61.
- [29] Savi MA, De Paula AS, Lagoudas DC. Numerical Investigation of an Adaptive Vibration Absorber Using Shape Memory Alloys. *J Intel Mat Syst Str*. 2011;22:67-80.
- [30] Williams KA, Chiu GTC, Bernhard RJ. Dynamic modelling of a shape memory alloy adaptive tuned vibration absorber. *J Sound Vib*. 2005;280:211-34.
- [31] Tian L, Liu J, Qiu C, Rong K. Temperature effect on seismic behavior of transmission tower-line system equipped with SMA-TMD. *Smart Structures and Systems*. 2019;24:1-14.
- [32] Poh'Sie GH, Chisari C, Rinaldin G, Amadio C, Fragiacomano M. Optimal design of tuned mass dampers for a multi - storey cross laminated timber building against seismic loads. *Earthquake Engineering & Structural Dynamics*. 2016;45:1977-95.

- [33] Sladek John R, Klingner Richard E. Effect of Tuned - Mass Dampers on Seismic Response. *J Struct Eng.* 1983;109:2004-9.
- [34] Huang H, Zhu Y-Z, Chang W-S. Comparison of Bending Fatigue of NiTi and CuAlMn Shape Memory Alloy Bars. *Advances in Materials Science and Engineering.* 2020;2020:1-9.
- [35] Xie W, Araki Y, Chang W-S. Enhancing the seismic performance of historic timber buildings in Asia by applying super-elastic alloy to a Chinese complex bracket system. *International Journal of Architectural Heritage.* 2018;12:734-48.
- [36] Nagarajaiah S, Varadarajan N. Novel semiactive variable stiffness tuned mass damper with real time tuning capability. In: Reston tEMC, editor. Virginia: ASCE; 2000.
- [37] Huang H, Chang W-S. Re-tuning an off-tuned tuned mass damper by adjusting temperature of shape memory alloy: exposed to wind action. *Structures.* 2020;25:180-9.
- [38] Warburton GB. Optimum Absorber Parameters for Various Combinations of Response and Excitation Parameters. *Earthquake Eng Struct.* 1982;10:381-401.
- [39] Sadek F, Mohraz B, Taylor AW, Chung RM. A method of estimating the parameters of tuned mass dampers for seismic applications. *Earthquake Eng Struct.* 1997;26:617-35.
- [40] Tsai HC, Lin GC. Optimum Tuned-Mass Dampers for Minimizing Steady-State Response of Support-Excited and Damped Systems. *Earthquake Eng Struct.* 1993;22:957-73.
- [41] Meirovitch L. *Fundamentals of vibrations.* Boston: McGraw-Hill; 2001.
- [42] Xie W, Wang T-H, Chang W-S. Static behaviour of a two-tiered Dou-Gong system reinforced by super-elastic alloy. *Proceedings of the Institution of Civil Engineers - Engineering History and Heritage.* 2019;172:164-73.
- [43] Tsiavos A, Stojadinović B. Constant yield displacement procedure for seismic evaluation of existing structures. *Bulletin of Earthquake Engineering.* 2019;17:2137-64.
- [44] Omori T, Kusama T, Kawata S, Ohnuma I, Sutou Y, Araki Y et al. Abnormal Grain Growth Induced by Cyclic Heat Treatment. *Science.* 2013;341:1500-2.
- [45] Araki Y, Maekawa N, Shrestha KC, Yamakawa M, Koetaka Y, Omori T et al. Feasibility of tension braces using Cu-Al-Mn superelastic alloy bars. *Struct Control Hlth.* 2014;21:1304-15.
- [46] Eggeler G, Hornbogen E, Yawny A, Heckmann A, Wagner M. Structural and functional fatigue of NiTi shape memory alloys. *Mat Sci Eng a-Struct.* 2004;378:24-33.
- [47] Soul H, Isalgue A, Yawny A, Torra V, Lovey FC. Pseudoelastic fatigue of NiTi wires: frequency and size effects on damping capacity. *Smart Mater Struct.* 2010;19.
- [48] Miyazaki S, Imai T, Igo Y, Otsuka K. Effect of cyclic deformation on the pseudoelasticity characteristics of Ti-Ni alloys. *Metall Trans A.* 1986;17:115-20.
- [49] Kawaguchi M, Ohashi Y, Tobushi H. Cyclic characteristics of pseudoelasticity of Ti-Ni alloys - (effect of maximum strain, test temperature and shape memory processing temperature). *Jsm Int J I-Solid M.* 1991;34:76-82.
- [50] Choi E, Nam TH, Chung YS. Variation of mechanical properties of shape memory alloy bars in tension under cyclic loadings. *Mat Sci Eng a-Struct.* 2010;527:4412-7.
- [51] Khan MI, Kim HY, Namigata Y, Nam TH, Miyazaki S. Combined effects of work hardening and precipitation strengthening on the cyclic stability of TiNiPdCu-based high-temperature shape memory alloys. *Acta Mater.* 2013;61:4797-810.